

- (77) Daubeny, R. de P.; Bunn, C. W.; Brown, C. J. *Proc. R. Soc. (A)* **1954**, *14*, 531.
 (78) Cunningham, A.; Manuel, A. J.; Ward, I. M. *Polymer* **1976**, *17*, 125.
 (79) Opella, S. J.; Waugh, J. S. *J. Chem. Phys.* **1977**, *66*, 4919.
 (80) Harbison, G. S.; Spiess, H. W. *Chem. Phys. Lett.* **1986**, *124*, 128.
 (81) Zilm, K. W., personal communication.
 (82) Swanson, S.; Ganapathy, S.; Kennedy, S.; Henrichs, P. M.; Bryant, R. G. *J. Magn. Reson.* **1986**, *69*, 531.

Analysis of Surface Structures in Nitrogen-Containing Polymer Systems by Ion Scattering Spectroscopy

Kevin J. Hook and Joseph A. Gardella, Jr.*

Department of Chemistry, State University of New York at Buffalo,
Buffalo, New York 14214

Lawrence Salvati, Jr.

Perkin Elmer Physical Electronics Laboratories, Edison, New Jersey 08820.

Received February 2, 1987

ABSTRACT: Low-energy ion scattering spectroscopy (LEIS or ISS) combined with molecular mechanics calculations is used to predict the structure and orientation of functional groups at the topmost surface for a group of nitrogen-containing polymers. ISS of poly(2-vinylpyridine) (P2VP), poly(4-vinylpyridine) (P4VP), and ethylated P2VP gives N/C scattered ion intensity ratios which reflect the position of the nitrogen in the planar side group. The N/C scattered intensity ratios were 0.404 ± 0.025 for P4VP, 0.01 ± 0.02 for P2VP, and 0.42 ± 0.025 for ethylated P2VP. Results are explained through the use of conformational energy calculations, classical concepts such as "shadowing" and "shielding" effects, and molecular modeling. X-ray photoelectron spectroscopy (XPS or ESCA) data show no differences between P2VP (ortho nitrogen) and P4VP (para nitrogen). ISS of poly(vinylpyrrolidone) (PVPyr) and poly(vinylcarbazole) (PVK) is used to complement the work done on the pyridine polymers. The combined data support a polymer orientation in which the polymer backbone is exposed to the vacuum at the vacuum/surface interface. These results are possible because of the extreme surface sensitivity of the ISS technique.

Introduction

ISS is a surface analytical technique which samples a shallow surface region (3–5 Å) and thus gives direct and indirect information on surface composition, structure, molecular orientation, and morphology.^{1,2} The principle behind ISS is quite straightforward. Typically, a monoenergetic beam of noble gas ions such as ³He, ⁴He, or ²⁰Ne is scattered from a surface with the energy of the scattered ion dependent upon the atomic composition of the surface. The energetics of the scattering event can be described by using the following equation which is derived from the laws of conservation of energy and momentum:¹

$$\frac{E_1}{E_0} = \frac{M_1^2}{(M_1 + M_2)^2} \left[\cos \theta + \left(\frac{M_2^2}{M_1^2} - \sin^2 \theta \right)^{1/2} \right]^2 \quad (1)$$

where E_0 and E_1 represent the energy of the ions before and after the scattering event, M_1 and M_2 represent the masses of the primary ion and of the surface atom, respectively, and θ is the laboratory scattering angle.

As Niehus and Comsa point out, sensitivity to the first atomic layer is due to the severe neutralization of the noble gas ions used in the ISS technique.³ Practically none of the incident ions that penetrate farther into the sample than the first layer are able to scatter into the vacuum as an ion. The high neutralization probability of the ion is the result of the occupation of an atomic state by a surface electron that occurs because of coupling to the solid. A noble gas ion incident with a surface presents a deep potential well for an electron (–24.6 eV for He, –21.6 eV for Ne, and –15.8 eV for Ar) compared with the work function of a solid (about 2–5 eV),^{4,5} the result being that during a scattering event the surface electron can neutralize the

incident ion. Charge capture largely occurs via both one-electron resonant and two-electron Auger processes, with the dominant process being highly dependent on the specific energetics of the ion–surface interaction.^{5–8}

The interaction between the incident ion and a surface atom results in the formation of areas which are effectively shielded from the possibility of undergoing a collision with the incoming ion beam. The interaction can be described classically through the use of a "shadow" cone.⁹ Because of the low-energy conditions used in this technique, incoming ions are scattered by a relatively weak potential which is effectively described by the screened Coulomb potential.^{1,9} As discussed in our previous paper,² "shielding" and "shadowing" represent two different conditions. The term shadowing means the situation when an atom heavier than ³He prevents ion scattering from atoms lying underneath. The term shielding in this case will describe the situation when an atom lighter than the primary ion slightly deflects or is sputtered by the primary ion. The slight deflection does not utilize hydrogen as the scattering center. However, as observed by Diehl,¹⁰ this prevents ion scattering from occurring and affects relative intensities.

It is important in ISS to address certain limitations which are inherent in the technique. Of primary concern is the difficulty in resolving spectral peaks which are broad and suffer from large overlap. Secondly, as can be seen in eq 1, the ISS method cannot detect elements lighter than ³He. However, weakly adsorbed hydrogen does produce inelastic scattering effects which are evident in the overall appearance of the spectrum, the result being a large background which further complicates spectral interpretation. Another limitation, the inability to obtain absolute primary ion intensities, will force reliance on relative ion intensity ratios to obtain quantitative information. Nevertheless, because of the extreme surface

* Author to whom correspondence should be addressed.

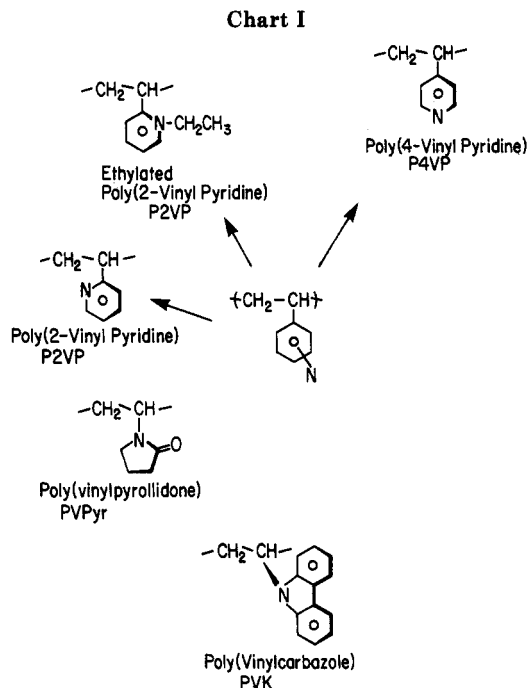
sensitivity of the technique, it can provide important advantages for a variety of applications. The use of ISS in polymeric analysis is an excellent example of the ability of the technique to extract surface-sensitive information.

A final consideration in ISS of polymer surfaces is the need to use "static" or "low-damage" conditions.^{11,12} During the ISS experiment sputtering of ions and neutrals from the surface occurs, therefore the use of static experimental conditions is very important in order to avoid excess surface damage to the polymer. Beam-induced changes to the surface structure are more important in polymers (and molecular-based surfaces) than for inorganic surfaces.^{2,11} This damage does not affect atomic intensities, but it can drastically change molecular and orientational information derived from the ISS spectra. To sacrifice static conditions will result in the loss of some of the main advantages of this analytical technique as applied to organic or polymer surfaces. Therefore, our primary concern in these studies will be in limiting surface damage, which in turn will allow us to derive molecular surface information from several structurally related polymers.

It has been demonstrated in previous work from this lab that ISS is sensitive to differences in surface structure and functional group arrangement due to tacticity in polymers.² Specifically, it was possible to differentiate between isotactic, syndiotactic, and atactic poly(methyl methacrylate) by comparing the C/O scattered ion intensity ratios obtained in the ISS experiment. The lower C/O ratio for syndiotactic PMMA as compared to isotactic PMMA is the result of the greater availability of the oxygen as a scattering center in the syndiotactic polymer. This was explained and illustrated through the use of molecular models. It was also shown that core-level ESCA data were not able to distinguish between the stereoregularity of the polymer surface. This result was expected due to the greater sampling depth of the ESCA technique and also as a result of all samples having the same atomic C/O ratio. The core-level results can be contrasted with the small differences in the valence band that would be expected and have been observed by Pireaux.¹³ Additionally no chemical shift differences were seen in the core-level data for the stereoregular PMMA's and none would be expected.

The work discussed in this paper has involved the study of a group of nitrogen-containing vinyl polymers with the nitrogen present in various positions of a cyclic side functionality. The present study focuses on the use of ISS to *predict* the actual position of the nitrogen in the ring by relating nitrogen position to the N/C scattered ion intensity ratios obtained in the experiment. Two important steps will be taken in order to enable us to model the polymer surface orientation. The first area involves the use of conformational energy calculations to predict favorable polymer side-chain orientations. Extensive calculations of minimum ring energies for several vinyl polymers with large planar side-chain substituents have been presented by Tonelli^{14,15} and Sundararajan.¹⁶ The studies involved the use of semiempirical potential energy functions appropriate to vinyl polymers in order to estimate their conformational energies. These calculations are for polymers in solution, but because of the large steric interference between side rings in these polymers, we assume similar orientations would be expected in the solid state. This assumption will in effect be verified by the ISS data presented in this paper.

The second step is the use of molecular models to obtain a qualitative understanding of polymer chain orientation at the surface. In our previous paper² molecular models were used to explain experimental results on the basis of



shadowing and shielding interactions consistent with the ISS data. Also, the work was centered on polymers with differences in stereoregularity and the ability of ISS to detect those variations. The present work focuses on orientation differences as a result of varying isomeric structure. This means we will be measuring orientational differences on the level of a few angstroms, differences that are a result of unique molecular alignment. Although the picture we derive from molecular modeling is at best an approximation, it will allow us to visualize the necessity for specific polymer orientations at the polymer/vacuum interface in order to explain experimental results. It is also possible to take advantage of the unique chemistry of these polymers to form a derivatized material. The result of such derivatization is a variation in the orientation of the large planar side group present in these polymers.

Experimental Section

Polymer Preparation. The polymers analyzed in this study were in their atactic form and are listed in Chart I. All polymers samples were analyzed as thick films on a silver substrate cast from $\approx 1\%$ (by weight) solutions. Chloroform was the solvent used for P2VP, P4VP, PVK, and PVPyr. The quaternization of P2VP was carried out in ethanol. Butyl bromide and ethyl bromide were added to the polymer which was previously dissolved in ethanol to form a $\approx 1\%$ solution. The solution-casting procedure involved pipetting 10–20 mL of the polymer solution into a petri dish containing silver coupons. The petri dish was covered and the solvent allowed to evaporate over a 72-h period at minimum. Before analysis, all samples were extracted by using a combined hexane/methanol extraction procedure. The coupon was ultrasonically cleaned in hexanes for ≈ 1 –2 min to remove surface contamination (especially from residual siloxanes) which has been shown to migrate to the surface.¹⁷ This was followed by extraction in methanol which was found to remove any surface oxidation or polar impurities (e.g., from original polymer synthesis) present after the casting procedure.¹⁸

Instrumentation. ISS spectra were recorded on a Physical Electronics Model 560 ESCA/SAM modified for ISS. A 2-kV beam of $^3\text{He}^+$ ions was utilized with a beam current density of $< 6 \text{ nA/cm}^2$, defocused, and rastered over $3 \times 3 \text{ mm}^2$ except where indicated. A 144° scattering angle and 90° sector of the CMA was used for analysis. Calibration was done by using polycrystalline Ag foil. Each ISS spectrum took approximately 2 min to acquire. Eight to ten consecutive spectra were obtained to estimate depth profiles and beam damage effects. Standard MACS

version 6 software was used for all analyses. Signals were processed as if Auger depth profiles were being acquired. Peak height ratios were used to interpret the ISS data due to the uncertain background,^{19,20} which results in difficulties with peak area ratios. To ensure low damage conditions, ESCA was performed before and after ISS analysis. The area of the ESCA nitrogen peak was ratioed to the area of the carbon peak before the ISS analysis. This procedure was repeated again after ISS analysis to verify that this ratio remained the same. A significant change in the ratio after ISS analysis would indicate severe damage to the sample surface. ESCA peak positions and peak shapes (evaluated by fwhm) were measured before and after ISS analysis to ensure there were no shifts in the binding energy or broadening of the peaks which would indicate chemical modification of the surface due to sputtering. No damage was detected by ESCA for any polymer sputtered for less than 5 min. Damage studies over the entire profile confirm, to the limits of ESCA detectability, that low-damage conditions are utilized and sensitivity to the topmost layer is accessible. For ISS analyses given here, only the first spectrum acquired in a profile was used. In order to estimate experimental error at a specific sputter time, profile measurements were repeated for a polymer sample approximately 6–8 times using separate Ag coupons supporting a fresh thick film of the polymer.

ESCA measurements were taken on a Physical Electronics PHI 5400 ESCA. The PHI instrument utilizes a 180° hemispherical analyzer with a position-sensitive detector. Mg K α X-rays were used as the source, operated at 300 W, 15.0 kV, and 20 mA. High-resolution scans were done at a pass energy of 18 eV, leading to a resolution on the Ag 3d_{5/2} line of 0.86 eV at 110 000 counts/s. A variable-angle sample stage (5–90°) was used. Data were acquired with a Perkin-Elmer 7500 professional computer fitted with a standard software package.

Molecular modeling was done with a commercially available software package on the IBM PC/AT. The modeling package used in this study was ChemCad software, which is a product of Daniel R. Kuhn and C-Graph Software, Inc., Austin, TX 78763. The ChemCad package also includes software to perform simple geometry optimization on the polymers under study. However, conclusions on the favorable conformational energies of the polymers in the solid state were based on the published theoretical data of Tonelli^{14,15} and Sundararajan¹⁶ for the same polymers in solution.

Results and Discussion

The first comparison will be made between ISS spectra for P2VP and P4VP (Chart I). The steric interactions of the side-chain substituent in the series of polymers used in the study is extremely important. All the polymers studied contain large planar side chains that are limited in rotational freedom because of steric considerations. Tonelli^{14,15} and Sundararajan¹⁶ have reported from molecular mechanics calculations a minimum-energy conformation for planar ring side chains in certain vinyl polymers. The planar side group is contained in a plane which lies perpendicular to the plane containing the polymer backbone (Figure 1). The steric effects would be assumed to be much the same for the P4VP polymer in comparison with P2VP. The ring nitrogen in P4VP is in the para position and should be available for scattering in all energetically favorable orientations of the planar side group. However, in P2VP the rotational position of the side group will result in the shadowing of the ring nitrogen which has been shown to lie preferentially beneath the polymer backbone.¹⁴ Because of shadowing effects, the spectra obtained from P2VP would be predicted to be quite different from that of P4VP. The geometry of both P2VP and P4VP can be visualized easier through the use of space-filling models (Figure 1 and 2). It can be seen that if the polymer backbone is exposed to the surface as contact angle measurements would suggest²¹ then the nitrogen will not be available as a scattering center in P2VP (Figure 2). If the polymer backbone is contained in the bulk of the polymer with the side groups exposed

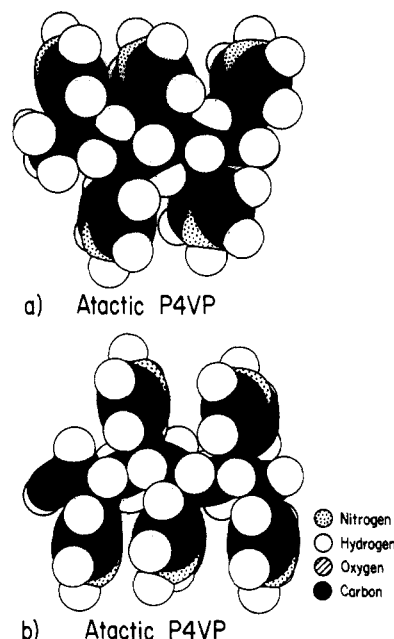


Figure 1. Space-filling model of a P4VP chain with (a) the polymer backbone exposed to vacuum and (b) the polymer backbone pointing into the bulk (note that in both orientations the nitrogen would be available for scattering).

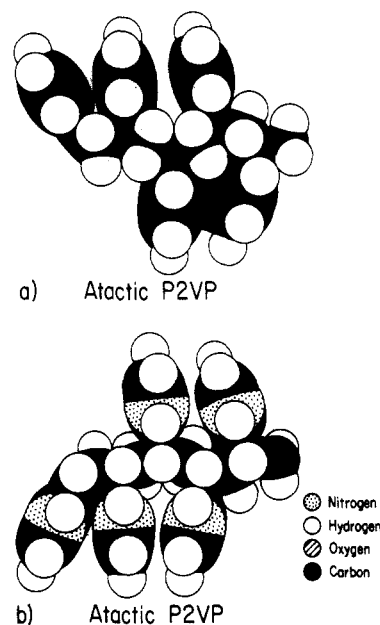


Figure 2. Space-filling model of a P2VP chain with (a) the polymer backbone exposed to vacuum at the vacuum/surface interface (notice the nitrogen is not visible) and (b) the polymer backbone pointing into the bulk (in this configuration the nitrogen would be available for scattering).

to the vacuum/surface interface, then nitrogen should be available for scattering. This can be contrasted with the space-filling models of P4VP which show that the ring nitrogen would be exposed to the vacuum/surface interface in either orientation of the polymer backbone (Figure 1). ISS spectra for P4VP were composed of peaks for carbon and nitrogen centered at 783- and 910-eV kinetic energy, respectively, corresponding to calculated energy ratios of 0.396 and 0.455, expected from 2-kV ³He⁺ scattering at 144°. However, initially only a peak at 793-eV kinetic energy corresponding to carbon was present in the ISS spectra for P2VP (Figure 3). The measured N/C ratios after 1.45 min of sputtering were 0.404 ± 0.025 for P4VP and 0.010 ± 0.020 for P2VP (Figure 4). As expected the

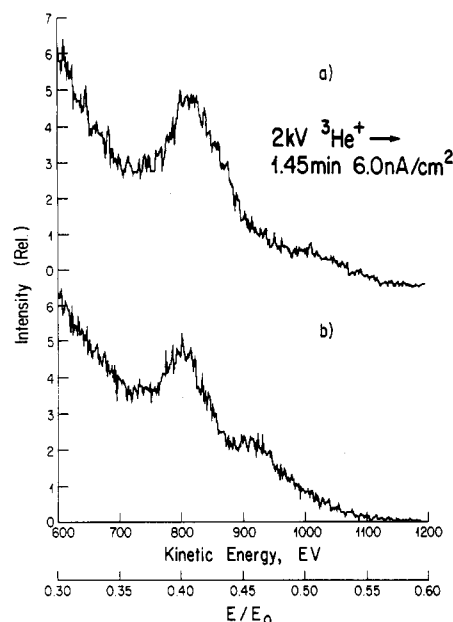


Figure 3. ISS spectra of poly(vinylpyridine) isomers (a) P2VP and (b) P4VP. The carbon peak is present at 783-eV kinetic energy and nitrogen peak at 910-eV kinetic energy.

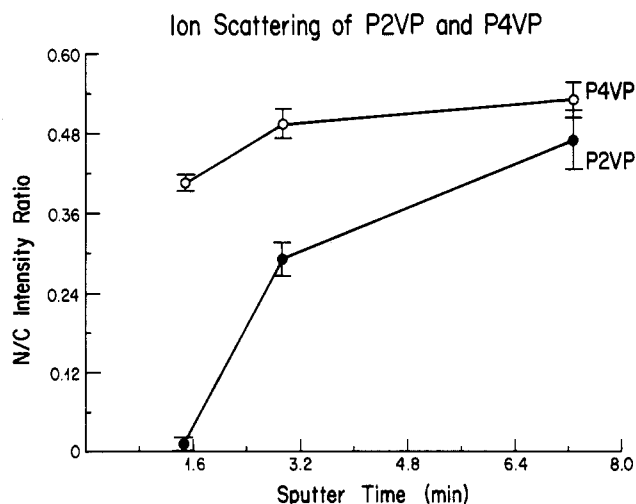


Figure 4. ISS scattering results show initial difference between P4VP and P2VP. The relative intensities coalesce after approximately 7 min.

nitrogen-scattering signal in P2VP is almost completely attenuated by the interference from the polymer backbone. This can only be explained if the backbone is somehow shielding the nitrogen from the incoming ion beam. The N/C scattered ion intensity ratio is significantly different for P4VP as we would have predicted. It is also interesting to notice that the N/C ratios for P2VP and P4VP coalesce after approximately 7 min, apparently the result of surface damage caused by continual sputtering. In summarizing this first area of study, it seems the ISS technique is sensitive enough to differentiate between atomic-level variations in isomeric polymer chains.

The next step we took was in applying the extreme surface sensitivity of the technique to a derivitized form of one of the first two systems we studied. The reason for this was the hope that ISS would be able to identify any type of side-chain rotation resulting from chemical modification. Specifically, both ethyl bromide and butyl bromide were added to a solution of $\approx 1\%$ (by weight) of P2VP in methanol. The result is the formation of a quaternary ammonium salt of the vinyl pyridine, with the

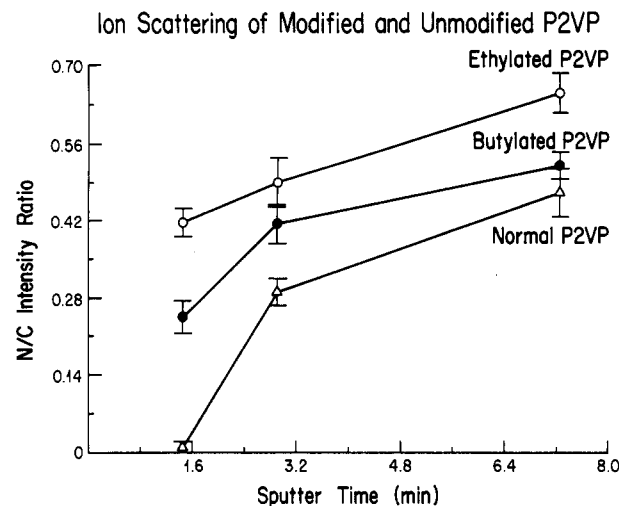


Figure 5. ISS scattering results shown for both modified and unmodified P2VP. Derivatization results in rotation of the side group and increased nitrogen availability for scattering.

addition of the alkyl group to the nitrogen in the ring structure²² (Chart I). One question is if steric and solvent interactions cause the vinyl pyridine ring in the derivitized polymer to rotate so that the nitrogen is no longer shielded by the hydrocarbon backbone. ISS analysis of the modified P2VP system yields contrasting results when compared with the unmodified P2VP and P4VP systems. ISS spectra for ethylated and butylated P2VP are comprised of peaks for carbon and nitrogen (Figure 5). In the case of the ethylated polymer, the initial scattering is similar to the value for P4VP and suggests a ring rotation which uncovers the nitrogen in the ortho position of ethylated P2VP. Butylated P2VP has a lower initial N/C intensity ratio than ethylated P2VP, roughly halfway between the unmodified and ethylated scattering intensities. This variation can be explained due to the difference in size between the two alkyl groups. The larger butyl group would shield the ring nitrogen more completely than the smaller ethyl group. The expected result would be a correspondingly lower nitrogen peak intensity in the spectra of the butylated polymer. Again, in both cases this would support the idea of a ring rotation that exposes the ortho ring nitrogen to the vacuum/surface interface allowing scattering of the incoming ions from nitrogen to occur.

Another important question to answer in studying these polymer systems is if the polymer backbone (vinyl portion) is exposed to the surface of the film. To answer this question we decided to combine the data from the polymers we had already studied with the ISS spectral data of poly(vinylcarbazole) (PVK) and poly(vinylpyrrolidone) (PVPyr) (Chart I). PVK has an extremely large planar side chain which should very effectively shield initial scattering from nitrogen because the nitrogen lies at the center of the multiple-ring structure (Figure 6). The low probability for scattering from the nitrogen would be the same whether the hydrocarbon backbone was oriented toward the bulk of the polymer or exposed at the vacuum/surface interface. Thus it would not be possible to derive the orientation of the chain by simply relying on this chain. However, we can test the initial visibility of the nitrogen to the incoming ion beam. It would be expected that the spectra for PVK would resemble the initial scattering environment of unmodified P2VP. The initial ISS spectra for PVK is comprised only of a peak for carbon with the nitrogen peak absent as expected (Table I). However, at 3 min the nitrogen has now become available

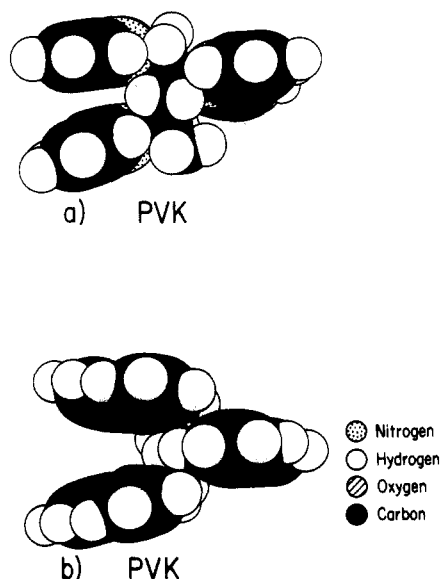


Figure 6. Space-filling model of a PVK chain with (a) the polymer backbone exposed to the surface and (b) the polymer backbone pointing into the bulk (note that in both orientations the nitrogen would not be available for scattering).

Table I
ISS Analysis of PVK and PVPyr

sample	N/C ratio ($\pm 10\%$)		O/C ratio ($\pm 10\%$) ^a	
	init scan	10-min sputter	init scan	10-min sputter
PVK	0.07 ± 0.06	0.46 ± 0.03	NA	NA
PVPyr	0.25 ± 0.05	0.59 ± 0.05	1.10 ± 0.09	0.41 ± 0.04

^a NA, not applicable to polymer system.

for scattering and a peak is visible in the ISS spectra. This is a result of surface damage caused by the ion beam and demonstrates the need for the use of low damage conditions as well as restricting ourselves to the use of the first scan (i.e., no signal averaging).

The final polymer system analyzed was that of poly(vinylpyrrolidone) (Chart I). The pyrrolidone ring is bonded to the vinyl group through the nitrogen, with an oxygen atom also part of the ring structure. This system has been studied by Tonelli¹⁵ with the conclusion that the oxygen atom is preferentially exposed as shown in Figure 7. This would lead us to suggest that there should be a large initial peak due to oxygen scattering in PVPyr, as well as a peak due to the nitrogen and one due to carbon. Our expectations are confirmed by the analysis which yields a strong scattering peak due to the oxygen present in the ring structure (Table I). One important point to make here is the necessary orientation of the polymer itself to allow for this type of scattering to occur. The polymer backbone must be exposed to the vacuum in order for an oxygen scattering peak to be observed in the initial spectra (Figure 7). Similarly, in reviewing earlier data, we can see that it is also necessary that the backbone be exposed in the case of both modified and unmodified P2VP in order to explain experimental data. It would be appropriate at this point to discuss the possibility of contamination at the surface of the polymer. There is a danger when using low-energy ISS that any signal measurement could have been mediated by selective hydrocarbon contamination. To eliminate this possibility we have used an extensive cleaning procedure and tested the effectiveness of this treatment by using angle-dependent ESCA as well as the ISS experimental results. In the presence of hydrocarbon

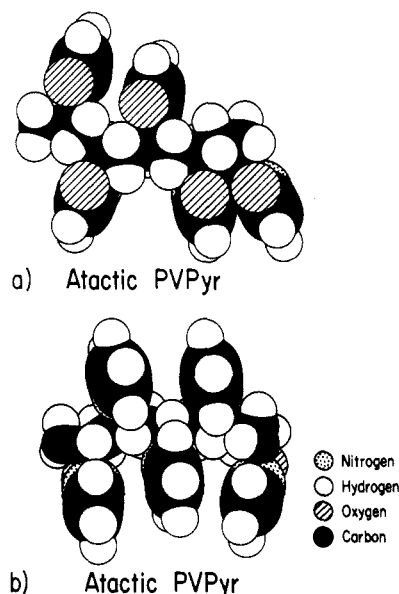


Figure 7. Space filling model of a PVPyr chain with (a) the polymer backbone exposed to the surface (oxygen available for scattering) and (b) the polymer backbone pointing into the bulk.

contamination it would be expected that the ESCA N/C peak area ratios would vary from sample to sample as we decrease the photoelectron takeoff angle and probe an area of the polymer that lies closer to the surface. Here we make the reasonable assumption that hydrocarbon contamination at the surface would not be consistent from sample to sample. In the present study all ESCA N/C peak area ratios remained constant as the takeoff angle was varied. The consistency in the N/C ratio would support the existence of a clean polymer surface. Further, the ISS N/C ratios were consistent (for a given time of sputter under equivalent beam conditions) as we measured them over a complete depth profile for a sample. The results shown in Figures 4 and 5 represent the average, with experimental standard deviation of six to eight samples run over a period of several months. Finally, the conclusions derived from these data are further supported by both contact angle²¹ and ESCA²³ measurements.

Conclusions

- (1) Nitrogen position in the planar side chain can be indirectly determined from N/C scattering intensity ratios.
- (2) In the case of P2VP and P4VP we can determine nitrogen position even though the bulk atomic N/C ratio was not different.
- (3) ISS is also sensitive to side-chain rotation that is the result of chemical derivitization of the polymer.
- (4) The combination of experimental results suggests a polymer orientation in which the backbone (vinyl portion) of the polymer chain is exposed to the surface.
- (5) The analytical technique of ISS is sensitive to structural differences in the extreme surface region (1–2 Å).

Acknowledgment. We thank Barbara E. Evans of the Educational Communications Center at SUNY at Buffalo for the construction of figures. We are also grateful to Dr. M. Aono of the Institute of Physical and Chemical Research and Dr. R. Souda of the National Institute for Research in Inorganic Materials for a preprint of their recent work. This work was supported by NSF Grant DMR 8412781 from the Polymers Program of the Division of Materials Research.

Registry No. P2VP, 25014-15-7; P4VP, 25232-41-1; PVK, 25067-59-8; PVPyr, 9003-39-8; P2VP butyl bromide, 28451-86-7; P2VP ethyl bromide, 30875-79-7.

References and Notes

- (1) Buck, T. M. In *Methods of Surface Analysis*; Czanderna, A. W., Ed.; Elsevier: Amsterdam, 1975; Chapter 3.
- (2) Hook, T. J.; Schmitt, R. L.; Gardella, J. A., Jr.; Salvati, L., Jr.; Chin, R. L. *Anal. Chem.* **1986**, *58*, 1285-1290.
- (3) Niehus, H.; Comsa, G. *Nucl. Instrum. Methods Phys. Res., Sect. B* **1986**, *B13*, 213-217.
- (4) Haeussler, E. N. *SIA, Surf. Interface Anal.* **1980**, *2*, 134-139.
- (5) Aono, M.; Souda, R. *Nucl. Instrum. Methods Phys. Res.*, in press.
- (6) Hentschke, R.; Snowdon, K. J.; Hertel, P.; Heiland, W. *Surf. Sci.* **1986**, *173*, 565-580.
- (7) Snowdon, K. J.; Hentschke, R.; Narmann, A.; Heiland, W. *Surf. Sci.* **1986**, *173*, 581-592.
- (8) Lee, H.; George, T. F. *Surf. Sci.* **1986**, *172*, 211-229.
- (9) Aono, M.; Souda, R. *Jpn. J. Appl. Phys.* **1986**, *24* (10), 1249-1262.
- (10) Diehl, J. R.; Stencel, J. M.; Spitler, C. A.; Makovsky, L. E. *SIA, Surf. Interface Anal.* **1980**, *18*, 2675.
- (11) Gardella, J. A., Jr.; Hercules, D. M. *Anal. Chem.* **1980**, *52*, 226.
- (12) Gardella, J. A., Jr.; Hercules, D. M. *Anal. Chem.* **1980**, *53*, 1879.
- (13) Pireaux, J. J. Laboratoire de Spectroscopie Electronique, Institute for Research in Interface Sciences, Facultes Universitaires, Belgium, personal communication, June 14, 1985.
- (14) Tonelli, A. E. *Macromolecules* **1985**, *18*, 2579-2583.
- (15) Tonelli, A. E. *Polymer* **1982**, *23*, 676-680.
- (16) Sundararajan, P. R. *Macromolecules* **1980**, *13*, 512-517.
- (17) Schmitt, R. L.; Gardella, J. A., Jr.; Magill, J. H.; Salvati, L., Jr.; Chin, R. L. *Macromolecules* **1985**, *18*, 2675.
- (18) Hook, K. J.; Gardella, J. A., Jr., unpublished observations, Sept 5, 1986.
- (19) Baun, W. L. *SIA, Surf. Interface Anal.* **1981**, *3*, 243.
- (20) Baun, W. L. In *Quantitative Surface Analysis of Materials*; McIntyre, N. S., Ed.; STP 643 ASTM; American Society for Testing and Materials: Philadelphia, 1978; pp 150-163.
- (21) Zisman, W. *Adv. Chem. Ser.* **1964**, *43*, 1.
- (22) Busch, K. L.; Unger, S. E.; Vincze, A.; Cooks, R. G.; Keough, T. *J. Am. Chem. Soc.* **1982**, *104*, 1507-1511.
- (23) Bigelow, R. W.; Bailey, F. C.; Salaneck, W. R.; Pochan, J. M.; Pochan, D. F.; Thomas, H. R.; Gibson, H. W. *Adv. Chem. Ser.* **1978**, *187*, 19.

CP/MAS ^{13}C NMR Spectra of the Crystalline Components of Native Celluloses

Fumitaka Horii,* Asako Hirai, and Ryozyo Kitamaru

*Institute for Chemical Research, Kyoto University, Uji, Kyoto 611, Japan.
Received November 18, 1986*

ABSTRACT: Cross-polarization/magic-angle-spinning (CP/MAS) ^{13}C NMR spectra of the crystalline components of different native celluloses have been measured in the hydrated state by using the difference in ^{13}C spin-lattice relaxation times $T_{1\rho}$ of the crystalline and noncrystalline components. As a result, it has been found that the crystalline spectra of native cellulose can be classified into two groups, cotton-ramie type and bacterial-valonia type, which are referred to as celluloses I_a and I_b , respectively. The validities of the structural models previously proposed have been also discussed on the basis of the line-shape analyses of the C1 and C4 triplets of the crystalline spectra.

Introduction

It is well-known that solid-state ^{13}C NMR spectra of cellulose exhibit two types of multiplicities: one is a large splitting on the order of 3-5 ppm, which is composed of a broad resonance and a narrow line, and the other is a fine splitting of less than 2 ppm appearing in the narrow line of the former splitting.¹⁻¹⁸ As a result of the evaluation of the effect of crystallinity on the former splitting, we have concluded that the narrow and broad resonances should be assigned to the contributions from the crystalline and noncrystalline regions.^{4,8} Although recent studies^{3,5,10} suggest that the surface chains on the crystallites also contribute to the broad component, this seems to be an overestimate of that contribution.

The origin of the fine multiplicities is also still a controversial subject. Atalla and VanderHart^{10,11} have proposed that all native celluloses are a mixture of two crystalline modifications, celluloses I_a and I_b , which show different fine multiplets. Analogous to their work, Cael et al.¹⁵ have also suggested that the ^{13}C NMR spectra of different native celluloses are linear combinations of two spectra. In contrast to the preceding view, however, these two spectra are assumed to correspond to the resonances from the two-chain and eight-chain unit cell regions of cellulose.

Although both models seem very interesting, these workers did not analyze any crystalline spectrum which was not contaminated with the noncrystalline contribution.

The situation is most serious for the C1 resonance, because a rather sharp line of the noncrystalline component is completely superposed on the central signal of the triplet ascribed to the crystalline contribution, as will be described later. Recently we have found that the ^{13}C spin-lattice relaxation times, $T_{1\rho}$, greatly differ for the crystalline and noncrystalline components, in accordance with the finding reported by Teeäär and Lippmaa,¹² and thus the pure spectra of the respective components can be separately recorded by using the difference in $T_{1\rho}$.^{8,9,13,14,18} Moreover, we have developed a new type of MAS rotor with an O-ring seal for CP/MAS ^{13}C NMR measurements in the presence of water.^{13,19} This kind of rotor is essential for cellulosic materials because the addition of water remarkably enhances the resolution of resonance lines and long-term measurements must be made without any loss of water to obtain the crystalline spectra with sufficiently high signal/noise ratios. In this paper, using these techniques, we have measured the crystalline spectra of cotton, ramie, bacterial, and valonia celluloses and compared their chemical shifts as well as multiplicities. As a result, we report that the ^{13}C crystalline spectra of these native celluloses are classified into two types, cotton-ramie type and bacterial-valonia type. The validities of the models previously proposed are also discussed.

Experimental Section

Each cellulose sample was prepared according to the methods reported in the previous papers.^{4,8} After being soaked in distilled